

A Simulation of the Process of High Speed Milling of Titanium Alloy VT-1-0 in DEFORM-3D

Karibek Sherov

S. Seifullin Kazakh Agrotechnical Research University (KATRU), 010011 Astana, Kazakhstan
k.sherov@kazatu.kz

Sayagul Tussupova

Toraighyrov University, 140008 Pavlodar, Kazakhstan
tussupova.s@teachers.tou.edu.kz (corresponding author)

Nadezhda Kuzminova

Karaganda Industrial University, 101400 Temirtau, Kazakhstan
n.kuzminova@tttu.edu.kz

Lutfiddin Makhmudov

Navoi State Mining and Technology University, 210100 Navoi, Uzbekistan
lmn_76@mail.ru

Bakhtiyor Mardonov

Navoi State Mining and Technology University, 210100 Navoi, Uzbekistan
mbt69@mail.ru

Saule Ainabekova

Karaganda Industrial University, 101400 Temirtau, Kazakhstan
s.ainabekova@tttu.edu.kz

Gulnur Abdugaliyeva

Abylkas Saginov Karaganda Technical University, 100027 Karaganda, Kazakhstan
g.abdugaliyeva@kstu.kz

Gulnara Kokayeva

S. Seifullin Kazakh Agrotechnical Research University (KATRU), 010011 Astana, Kazakhstan
g.kokaeva@kazatu.edu.kz

Saule Mendaliev

S. Seifullin Kazakh Agrotechnical Research University (KATRU), 010011 Astana, Kazakhstan
sauledecanuf2020@gmail.com

Sayat Kardassinov

S. Seifullin Kazakh Agrotechnical Research University (KATRU), 010011 Astana, Kazakhstan
s.kardasinov@kazatu.kz

Received: 23 June 2025 | Revised: 18 August 2025 | Accepted: 22 August 2025

Licensed under a CC-BY 4.0 license | Copyright (c) by the authors | DOI: <https://doi.org/10.48084/etasr.12892>

ABSTRACT

This study examined the High-Speed Milling (HSM) process of titanium alloy VT-1-0 using the Deform-3D simulation software. The simulation modeled the HSM operation and analyzed the distribution of temperature and strain in the cutting zone. The results indicated that deformation primarily occurred at the tool-workpiece interface and propagated more intensely into the sheared material at an angle of approximately 45°. Increasing the spindle speed of the end mill led to greater strain values in the cutting zone. Due to the low thermal conductivity of titanium, high temperatures-exceeding 1500 °C were localized at the tool-workpiece contact area. This concentration of heat, coupled with its slow dissipation throughout the workpiece, negatively affected the surface quality and tool life. Additionally, increasing both the feed rate and cutting speed resulted in higher temperatures and intensified friction at the interface.. The findings of this simulation provided valuable insights for optimizing the cutting parameters and better understanding the machinability of titanium under HSM conditions.

Keywords-High-Speed Milling (HSM); titanium machinability; modeling; deformation; temperature; cutting parameters

I. INTRODUCTION

The process of machining difficult-to-cut materials remains a challenge for many domestic industries, resulting in high material consumption and low productivity. Titanium alloys are among the most problematic materials in this category, exhibiting poor machinability. This can be attributed to the low thermal conductivity, high tendency for adhesion and built-up edge formation, intermittent cutting during milling, and low vibration resistance due to the instability in the plastic deformation process [1].

HSM is proposed as a possible solution for machining difficult-to-cut materials. Authors in [2] investigated the effects of HSM of Ti-6Al-4V titanium alloy using Physical Vapor Deposition (PVD) coated cutting plates. The results demonstrated that properties, such as good resistance to plastic deformation and impact fatigue failure, affected the wear resistance of the cutting tool, which led to an increase in its service life.

Multiple studies [3-6] examined the interdependent impact of cutting parameters - including tool wear, cutting forces, spindle speed, and machining vibrations - in HSM of difficult-to-cut materials. Specifically, in [3], the tool wear parameter was evaluated. As the cutting speed increased up to 190 m/min, the temperature raised, causing material heating and reduction of the friction coefficient, whereas above this speed, rapid edge wear occurred. Additionally, in [4], the progressive wear of the cutting edge led to a significant increase in the cutting forces and vibrations, which negatively affected the machine performance. Authors in [5, 6] conducted experiments on HSM of titanium alloys using different cutter types. In [5], self-propelled rotary tools were utilized in titanium milling, analyzing both the wear mechanisms and cutting speed effects on the process dynamics. The results demonstrated that increased milling speeds reduced cutting efficiency while accelerating tool wear rates. In [6], respectively, the cutting characteristics of TC11 were compared with rotary cycloidal cutter and spherical end mill. The wear zone of the rotating cycloidal cutter was shallow and wide compared to that of the spherical end mill. As wear accelerated, the spoon-shaped wear collection zone found in the spherical end mill did not occur in the rotary cycloidal cutter.

HSM investigations have been also extended to different difficult-to-cut materials. For instance, in [7], the effectiveness of using sialon ceramic milling tools for machining the nickel-based superalloy FGH96 was assessed, analyzing the cutting forces, thermal conditions, and tool wear. Authors in [8], examined the effect of the cutting speed on the surface roughness during the machining of super duplex stainless steel, while authors in [9] conducted a multi-objective optimization of the cutting parameters in the machining of Cr15Mo alloyed cast iron achieving a surface quality comparable to that of grinding. Particular attention was also given to the thermal effects in the cutting zone, as demonstrated in [10], where the machining of 30KhGSA and VT9 alloys was investigated. Additionally, in [11], various machining strategies for shafts made of VT1-10 titanium alloy were analyzed, and the optimal method of high-speed climb milling was identified. Authors in [12], demonstrated the positive effect of cutting fluid on the machining quality of hardened tool steel JIS SKD61.

Despite these advances, the implementation of HSM in domestic machine-building industries was not feasible due to the lack of next-generation high-speed metal-cutting equipment, such as machining centers and CNC semi-automatic machines. Until now, most domestic enterprises relied on machine tools manufactured by foreign companies, such as Victor Taichung (Taiwan), KAPP Niles (Germany), DOOSAN (South Korea), and MODUL (Germany).

The emergence of such machine tools with advanced technological capabilities enables the application of more efficient machining methods, such as HSM. However, this area remains less explored compared to other machining techniques. One of the existing challenges is the selection of the appropriate cutting parameters depending on the workpiece material and the tool material. Reference data for determining the cutting conditions at high spindle speeds (e.g., 5000 - 12000 rpm) are still limited, as the conventional machine tools were incapable of operating at spindle speeds exceeding 2000 rpm [13-15].

The aim of the present study is to investigate the thermal and deformation processes occurring during HSM using the specialized computer software DEFORM-3D.

II. MODELING OF THE HSM PROCESS OF VT1-10 TITANIUM ALLOY

Modeling is an essential part of the engineering analysis, with the Finite Element Method (FEM) considered as one of the most applicable tools for solving complex tasks. Particularly, through simulation, the cutting forces, chip morphology, stresses, strains, and temperatures can be predicted before the machining process. For example, authors in [16] simulated the milling conditions for medium-carbon steel AISI 1045 using an end mill and concluded that the quality characteristics of the milling process in 3D modeling depended on the selected material, tool geometry parameters, machining conditions, and the material model applied.

In the present study, a numerical simulation of titanium machining under face milling conditions was carried out in order to determine the deformations, stresses, cutting temperature, and tool wear using the DEFORM-3D software package.

DEFORM-3D is an effective tool for cost-efficient prediction of material consumption during forming processes in industry, as well as for minimizing the time delays associated with shop floor trials [17].

The material selected for the plane strain machining simulation was VT1-0 titanium, with a Brinell hardness of 160 HB, equivalent to Grade 2 titanium [18]. VT1-0 titanium combines high strength with good ductility and toughness. However, its low thermal resistance makes it less suitable for aerospace applications compared to specialized titanium alloys. Instead, it is more commonly used in the chemical industry due to its high corrosion resistance.

The face milling cutter used in the simulation was equipped with tungsten carbide (WC) inserts with a PVD coating. The technical specifications were: cutter diameter - 80 mm and number of carbide cutting inserts - 8. Figure 1 illustrates the milling cutter and workpiece modeled in DEFORM-3D with the applied mesh.

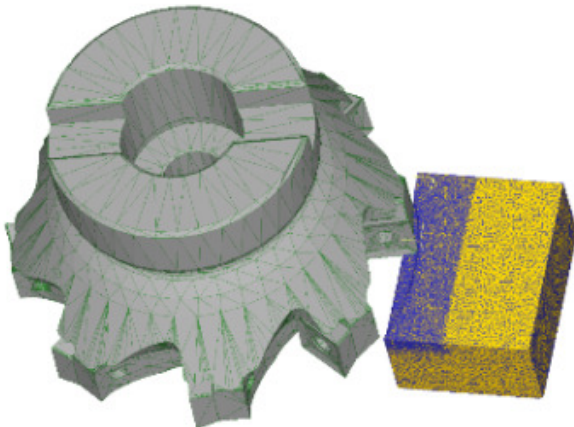


Fig. 1. Simulated milling cutter and workpiece using DEFORM-3D.

For the heat transfer and deformation calculations, a finite element tetrahedral mesh with automatic rearrangement at distortion $\geq 20\%$ was applied. The area between the workpiece

and the cutting edge, contained a finer mesh. The initial temperature of the workpiece, tool, and environment was set at 20 °C. The heat transfer coefficient between the workpiece and air was 20 W/(m °C). The model boundary conditions assumed that the workpiece was rigidly fixed, while the cutter moved only along the cutting axis at a spindle speed of 12,000 rpm, cutting depth of 1 mm, and feed rate of 4,500 mm/min.

The chemical composition of VT1-0 titanium, used as the workpiece material, is presented in Table I.

TABLE I. CHEMICAL COMPOSITION OF VT1-0 TITANIUM ALLOY ACCORDING TO GOST 19807-91

Fe	C	Si	N	Ti	O	H	Impurities
≤ 0.25	≤ 0.07	≤ 0.1	≤ 0.04	99.24 – 99.7	≤ 0.2	≤ 0.01	Other 0.3

The Johnson-Cook model, which characterizes the plastic deformation [19], was used:

$$\sigma_s = (A + B\varepsilon^n) \left(1 + C \cdot \ln \left(\frac{\dot{\varepsilon}}{\dot{\varepsilon}_0} \right) \right) \left(1 - \left(\frac{T - T_0}{T_m - T_0} \right)^m \right) \quad (1)$$

where:

- ε = accumulated deformation of the workpiece material
- $\dot{\varepsilon}$ = average deformation rate in the cutting area
- T = average temperature of the workpiece material in the cutting area
- T_m and T_0 = melting point and reference temperature of the workpiece material ($T_0 = 20\text{ °C} / 293\text{ K}$)
- $\dot{\varepsilon}_0$ = reference strain range
- $A, B, n, C,$ and m = coefficients obtained as a result of the statistical processing of the experimental data on the strength characteristics of the workpiece material. The initial yield stress was denoted by A , the hardening modulus by B , the strain hardening exponent by n , and the strain rate sensitivity coefficient by C .

The Johnson-Cook model parameters for titanium are displayed in Table II.

TABLE II. JOHNSON-COOK MODEL PARAMETERS FOR TITANIUM ALLOY

A	B	n	C	m
120	895	0.39	0.0066	0.85

The viscoplastic hardening parameter C was determined using data obtained from tensile testing, which inherently reflected the effects of strain hardening.

DEFORM includes a built-in database with dependencies, such as elastic modulus - temperature, yield strength - strain for different strain rates and temperatures, as well as heat capacity and thermal conductivity [19].

The Cockcroft-Latham fracture criterion [20] was also applied, representing the cumulative damage as [21, 22]:

$$\int_0^{\varepsilon_f} \sigma_{max} d\varepsilon = C_1 \quad (2)$$

where σ_{max} is the maximum main voltage, ε is the equivalent deformation, ε_f is the equivalent deformation in which fracture occurs, and C_1 is the constant of the material in case of plastic damage.

The wear rate on the contact surface was determined by the relative velocity, constant pressure, and absolute temperature in the Usui tool wear model:

$$\frac{d\omega}{dt} = A\sigma_u V_s e^{\left\{-\frac{B}{T}\right\}} \quad (3)$$

where $A = 0.0000000078$ and $B = 5,302$ [16].

III. SIMULATION RESULTS

The temperature and deformation distribution during the HSM of titanium were analyzed using a face milling cutter. Figure 2 illustrates the temperature distribution within the workpiece.

Models of workpieces with temperature and deformation distributions obtained in DEFORM 2D/3D were imported into Compass 2D. Using this program, the distances between the temperature and deformation boundaries were measured to determine the depth of distribution depending on the interval of indicators.

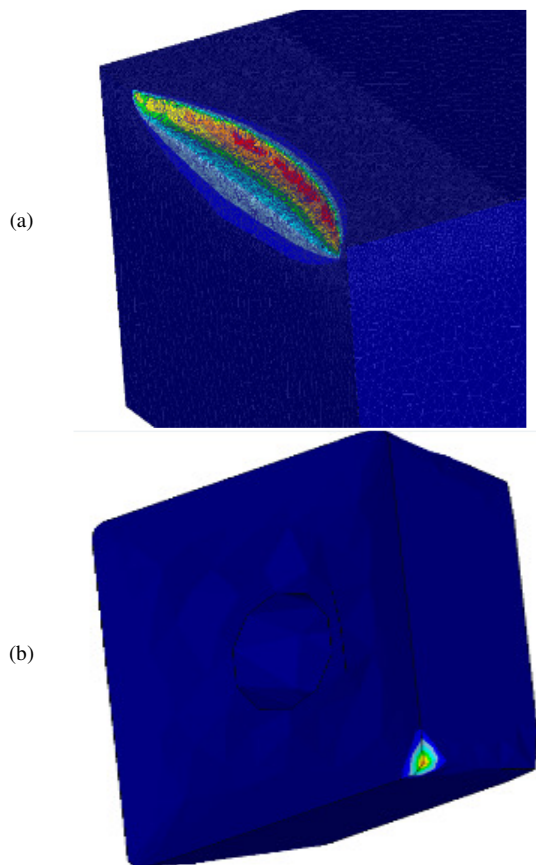


Fig. 2. Temperature distribution within the workpiece (a) and in the carbide cutting insert of the milling tool (b) during simulation.

The degree of final metal deformation was assessed by the magnitude of the relative shear strain. Deformation accumulates along the direction of the tool movement and is most pronounced at the end face of the workpiece, indicating its dependence on the cutting forces and chip separation. The values of equivalent strain provide insight into the degree of work hardening in the surface layer. Figure 3 portrays the distribution of strain in the cutting zone and throughout the body of the workpiece, and Figure 4 depicts the change of the cutting force.

According to Figure 4, the cutting force reached up to 500 kN during each spindle revolution. Sudden fluctuations in the force were observed due to remeshing of the FEM and chip formation resulting from the shearing of the metal layer. These moments corresponded to peak stress values, and the temperature in the cutting zone reaches up to 3000 °C.

The study of heat transfer processes in technological systems involves measuring temperatures at various locations of the tool, workpiece, or equipment, as well as determining the power and density of the heat fluxes. Such experiments are essential both for solving specific practical problems and for validating and refining theoretical models used to calculate the temperature distributions or characterize the heat sources and sinks. Numerous scientific and practical studies have focused on the problem of heat distribution in the cutting tool and the workpiece. However, the surface quality and tool wear are strongly influenced by the distribution of the thermal stresses along the cutting edge. Therefore, the temperature field modeling in this area can provide critical data for optimizing the cutting process and for the development of advanced tool materials.

In this simulation, it was possible to predict the generated heat and the resulting temperature distribution within the workpiece. Figure 5 presents the temperature distribution in the cutting zone and throughout the body of the workpiece after ten revolutions of the milling cutter.

Each tooth of the milling cutter remained in contact with the workpiece for approximately 0.005 s. During this time, the temperature within the workpiece increased on average by 90 °C. The temperature variation under different spindle speeds clearly revealed that, under initial cutting conditions, a sharp temperature rise occurred due to the intense friction between the cutting tool and the workpiece, caused by the shear interaction at the tool–workpiece interface. At lower feed rates, the contact pressure between the workpiece and the cutting tool decreased, resulting in a lower cutting temperature. However, at higher feed rates, the pressure tended to increase, which subsequently led to a rise in the cutting temperature. A similar trend was observed with an increasing depth of cut, where higher temperatures were also recorded [16].

To validate the simulation results, HSM of VT-10 titanium alloy was performed using a 90° face milling cutter equipped with AX14-type tungsten carbide (WC) inserts coated with PVD (Figure 6).

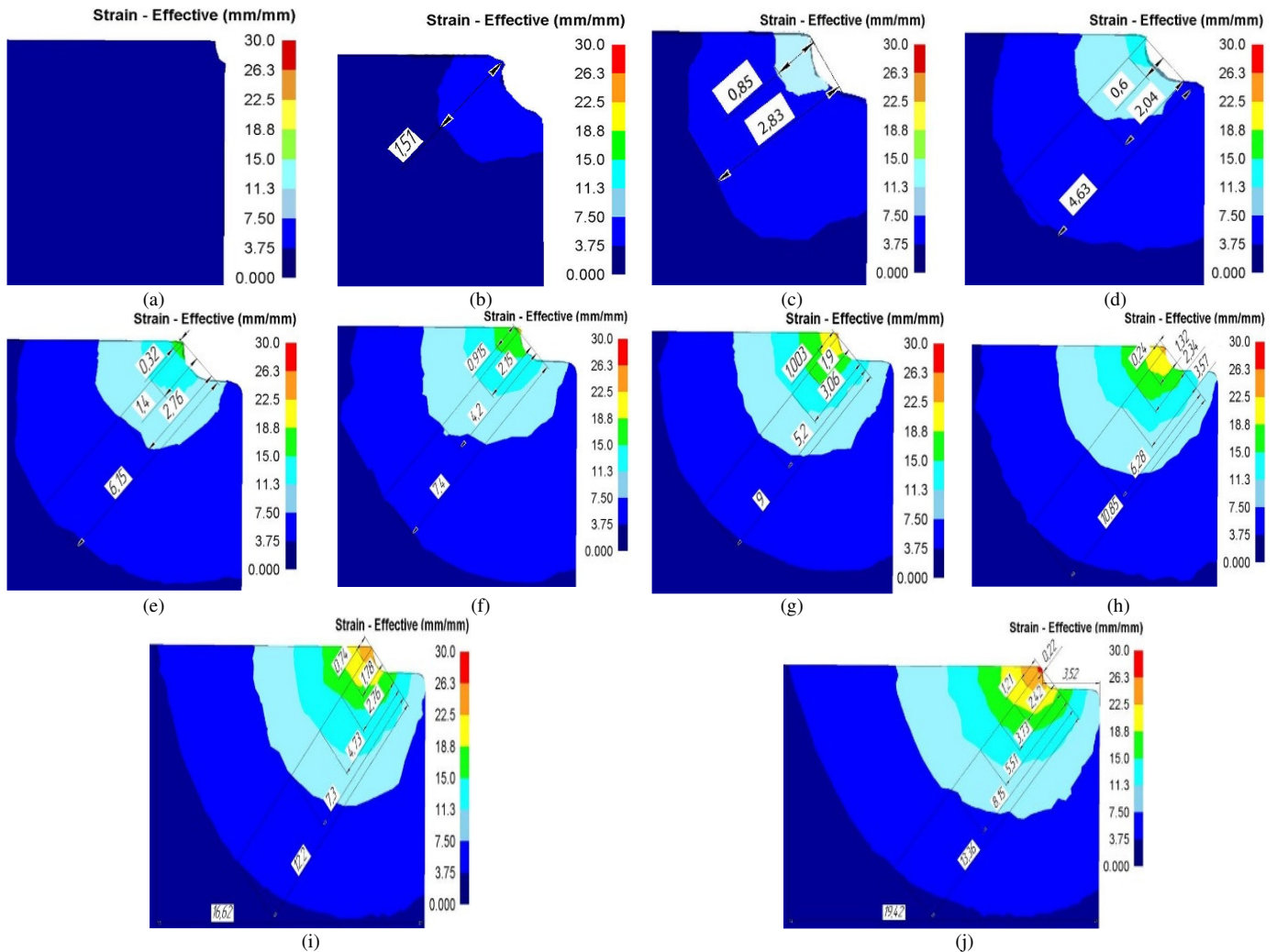


Fig. 3. Distribution of effective deformation: (a) 1 milling cutter turnover, (b) 2 milling cutter turnover; (c) 3 milling cutter turnover, (d) 4 milling cutter turnover, (e) 5 milling cutter turnover, (f) 6 milling cutter turnover, (g) 7 milling cutter turnover, (h) 8 milling cutter turnover, (i) 9 milling cutter turnover, (j) 10 milling cutter turnover.

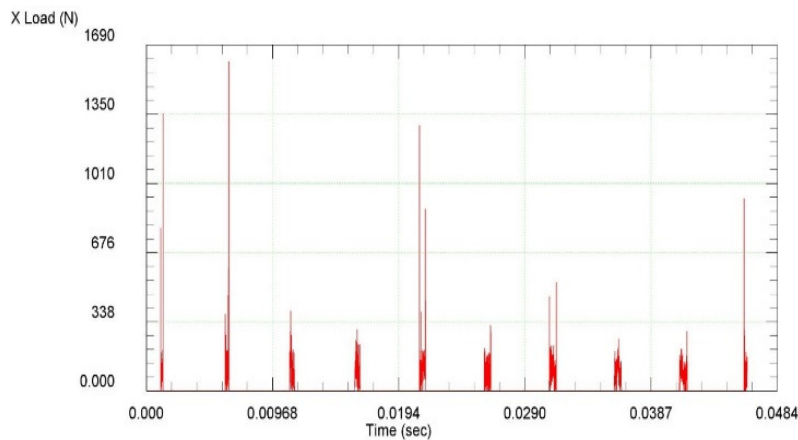


Fig. 4. Changing the cutting force.

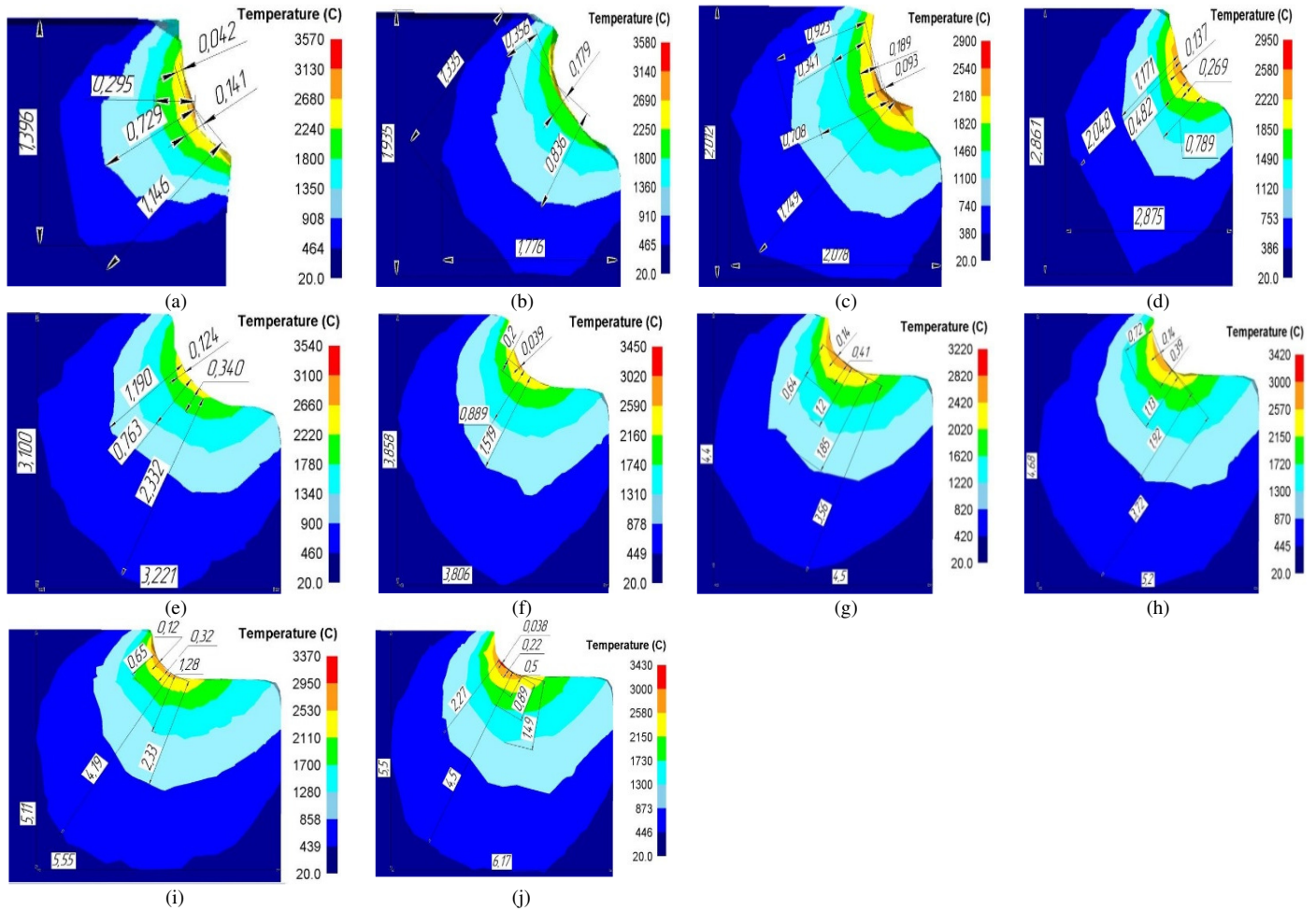


Fig. 5. Temperature distribution in the workpiece: (a) 1 milling cutter turnover, (b) 2 milling cutter turnover, (c) 3 milling cutter turnover, (d) 4 milling cutter turnover, (e) 5 milling cutter turnover, (f) 6 milling cutter turnover, (g) 7 milling cutter turnover, (h) 8 milling cutter turnover, (i) 9 milling cutter turnover, (j) 10 milling cutter turnover.



Fig. 6. Face milling cutter

The experiments were carried out on a vertical CNC machining center (V-Center P76) (Figure 7).

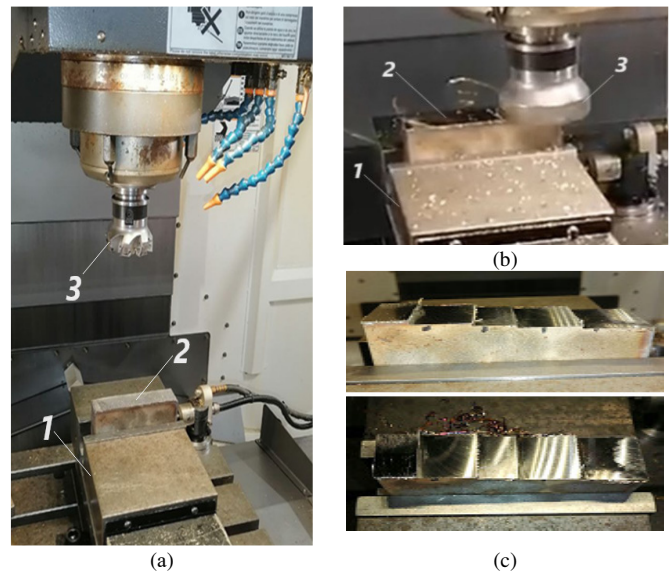


Fig. 7. HSM processes of VT1-10 titanium alloy: (a) setup of the V-Center P76 machining center, (b) HSM process, (c) titanium sample surfaces machined under different cutting conditions.

IV. DISCUSSION

Considering the equivalent deformations accumulated in the body of a titanium workpiece during face milling (Figure 3), it was observed that at the second revolution, the deformation values ranged from 3.75 to 7.5 to a depth of 1.51 mm (Figure 3(b)). At the following revolutions, the deformation values increased reaching a value of 9 to a depth of 0.85 mm in the tool-workpiece contacting zone (Figure 3(c)). It can be seen that deformations occurred at the tool-workpiece interface, while spreading more in the cut-off part of the workpiece at an angle of 45° (Figures 3(d)-3(j)).

The analysis showed (Figures 3(e), 3(f)), that the propagation depth of deformations ranging from 15 to 18.8 increased from 0.32 to 0.915, and later to 1.19 from the contact surface (Figure 3(g)). After 10 cutter revolutions, the deformation value reached 26 to a depth of 0.22 mm in the tool-workpiece contact. With each rotation of the cutter, the values of the deformations increased. At the same time, stresses accumulated to a depth of up to 13.36 mm, with a maximum value of 7.5.

When modeling the titanium milling process, the temperature inside the workpiece reached up to 3000 °C (Figure 5). On average, the temperature in the contact area did not exceed 2600 °C. Since the melting point of titanium is about 1600 °C, the elevated temperature indicated the rapid removal of metal particles from the cutting zone in the form of molten metal droplets or sparks.

As expected, the milling temperature spread with each revolution, dissipating heat deep into the workpiece. After the first revolution, the heat reached a depth of 1.4 mm with at 500 °C (Figure 5(a)). During subsequent rotations, the heat extended to a depth of 2 mm at the same temperature (Figures 5(b) and 5(c)). The heat accumulation increased with continued milling, raising the heating zone thickness to 0.137 mm at 2300 °C (Figure 5(d)), while the cut-off part heated up less (Figures 5(e) and 5(f)). When considering temperatures up to 800 °C, it can be seen that the depth of its propagation was not large (Figures 5(f)-5(j)). At the same time, the localization of temperature above 1000 °C practically did not change and was about 1.0 - 1.5 mm (Figures 5(f)-5(h)). Due to the low thermal conductivity of titanium, the localization of high temperatures above 1500 °C was located at the contact with the instrument. Consequently, the occurrence of a large amount of heat in the contact zone of the tool with the workpiece and its slow dissipation in the workpiece affected the tool wear and the quality of machining.

These findings aligned with those of previous studies on the HSM of titanium alloys [22, 23]. However, the present study provided, for the first time, a detailed quantitative analysis of the depth and intensity of deformation and temperature fields for commercially pure titanium VT1-0.

V. CONCLUSIONS

This study combined Finite Element Modeling (FEM) in DEFORM-3D with experimental validation to investigate the High-Speed Milling (HSM) of VT1-0 titanium alloy. Special

attention was placed to the distribution of temperature and deformation in the cutting zone.

The results provided some key insights:

- The analysis of deformation propagation revealed that deformation occurred at the tool-workpiece interface and spread in the cut-off part of the workpiece at an angle of 45°. With increasing cutter revolutions, the deformation value increased, reaching 26 at the tenth revolution with a depth of 0.22 mm in the "tool-workpiece" contact.
- Due to the low thermal conductivity of titanium, the localization of high temperatures above 1500 °C was located in the "tool-workpiece" contact area. The peak temperatures in the cutting zone reached ~ 3000 °C, while the average contact temperature did not exceed 2600 °C.
- The occurrence of a large amount of heat in the contact zone of the tool with the workpiece and its slow dispersion through its body had a negative effect on the quality of processing and on the durability of the tool.

Further research should focus on the prediction of tool wear and optimal processing parameters.

ACKNOWLEDGMENT

This research was funded by the Science Committee of the Ministry of Science and Higher Education of the Republic of Kazakhstan, Grant No. AP19174917-"Research and improvement of the quality of HSM of hard-to-process materials by modeling the process and optimizing cutting modes."

REFERENCES

- [1] H. A. Kishawy and A. Hosseini, *Machining Difficult-to-Cut Materials: Basic Principles and Challenges*. Cham, Switzerland: Springer International Publishing, 2019.
- [2] Q. He *et al.*, "Enhancing Tool Performance in High-Speed End Milling of Ti-6Al-4V Alloy: The Role of AlCrN PVD Coatings and Resistance to Chipping Wear" *Journal of Manufacturing and Materials Processing*, vol. 8, no. 2, Mar. 2024, Art. no. 68, <https://doi.org/10.3390/jmmp8020068>.
- [3] J. Matuszak, K. Zaleski, and A. Zyśko, "Investigation of the Impact of High-Speed Machining in the Milling Process of Titanium Alloy on Tool Wear, Surface Layer Properties, and Fatigue Life of the Machined Object," *Materials*, vol. 16, no. 15, July 2023, Art. no. 5361, <https://doi.org/10.3390/ma16155361>.
- [4] Z. J. Zhu, J. Sun, and L. X. Lu, "Research on the Influence of Tool Wear on Cutting Performance in High-Speed Milling of Difficult-to-Cut Materials," *Key Engineering Materials*, vol. 693, pp. 1129–1134, May 2016, <https://doi.org/10.4028/www.scientific.net/KEM.693.1129>.
- [5] L. Yujiang and C. Tao, "Research on cutting performance in high-speed milling of TC11 titanium alloy using self-propelled rotary milling cutters," *The International Journal of Advanced Manufacturing Technology*, vol. 116, no. 7, pp. 2125–2135, July 2021, <https://doi.org/10.1007/s00170-021-07592-4>.
- [6] G. Wang, X. Liu, T. Chen, and W. Gao, "An Experimental Study on Milling Titanium Alloy with a Revolving Cycloid Milling Cutter," *Applied Sciences*, vol. 10, no. 4, Feb. 2020, Art. no. 1423, <https://doi.org/10.3390/app10041423>.
- [7] W. Ming, X. Huang, M. Ji, J. Xu, F. Zou, and M. Chen, "Analysis of cutting responses of Sialon ceramic tools in high-speed milling of FGH96 superalloys," *Ceramics International*, vol. 47, no. 1, pp. 149–156, Jan. 2021, <https://doi.org/10.1016/j.ceramint.2020.08.118>.

- [8] L. Janardhan, K. Chandrappa, and R. Suresh, "An Experimental Study on High-Speed Milling of Super Duplex Stainless Steel and to Investigate the Effect of Cutting Parameters on Surface Roughness," *Journal of The Institution of Engineers (India): Series D*, vol. 105, no. 1, pp. 127–132, 2024, <https://doi.org/10.1007/s40033-023-00456-z>.
- [9] D. Maohua, J. Junhua, and J. Jianwei, "Robust Design Optimization Analysis of Experimental Results for High-Speed Milling of Alloy Cast Iron," *China Mechanical Engineering*, vol. 30, no. 5, 2019, Art. no. 554, <https://doi.org/10.3969/j.issn.1004-132X.2019.05.008>.
- [10] V. N. Trusov, D. L. Skuratov, O. I. Zakonov, and V. V. Shikin, "Calculation of Cutting Temperature at Milling of Purveyances from Hard-Processing Materials," *Bulletin of the Samara State Aerospace University*, vol. 27, no. 3, pp. 57–62, 2011, <https://cyberleninka.ru/article/n/vliyanie-rezhimov-rezaniya-na-temperaturu-pri-frezerovanii-zagotovok-iz-trudnoobrabatyvaemyh-materialov/viewer>.
- [11] A. N. Sellvanov and T. G. Nasad, "The Quality Maintenance of Processing Shafts From Titanium Alloys by High-Speed Milling and Turn-Milling Methods," *Bulletin of the Saratov State Technical University*, pp. 55–61, 2010, <https://cyberleninka.ru/article/n/obespechenie-kachestva-obrabotki-valov-iz-titanovyh-splavov-metodom-vysokoskorostnogo-frezerovaniya-i-frezotocheniya/viewer>.
- [12] T. H. Le, V. B. Pham, and T. D. Hoang, "Surface Finish Comparison of Dry and Coolant Fluid High-Speed Milling of JIS SDK61 Mould Steel," *Engineering, Technology & Applied Science Research*, vol. 12, no. 1, pp. 8023–8028, Feb. 2022, <https://doi.org/10.48084/etasr.4594>.
- [13] L. I. Vereina and M. M. Krasnov, *Machine Operator's Handbook: A Textbook for Initial Vocational Education*. 2nd ed., Moscow, Russia: Moscow Publishing Center "Academy," 2008.
- [14] B. I. Cherpakov and L. I. Vereina, *Technological Equipment of Machine-Building Production: A Textbook for Students of Secondary Vocational Education Institutions*, 6th ed. Moscow, Russia: Moscow Publishing Center "Academy," 2015.
- [15] S. O. Tusupova and L. N. Makhmudov, "State of the Problem of Processing Hard-to-Machine Materials," *Science and Technology of Kazakhstan*, no. 3, pp. 71–83, 2023, <https://doi.org/10.48081/GZVJ4547>.
- [16] B. Deepanraj, N. Senthilkumar, G. Hariharan, T. Tamizharasan, and T. Tefera Bezabih, "Numerical Modelling, Simulation, and Analysis of the End-Milling Process Using DEFORM-3D with Experimental Validation," *Advances in Materials Science and Engineering*, vol. 2022, no. 1, 2022, Art. no. 5692298, <https://doi.org/10.1155/2022/5692298>.
- [17] A. Mathivanan, G. Swaminathan, P. Sivaprakasam, R. Suthan, V. Jayaseelan, and M. Nagaraj, "DEFORM 3D Simulations and Taguchi Analysis in Dry Turning of 35CND16 Steel," *Advances in Materials Science and Engineering*, vol. 2022, no. 1, 2022, Art. no. 7765343, <https://doi.org/10.1155/2022/7765343>.
- [18] S. V. Kozlov and E. O. Shirshov, "Increasing the Efficiency of High-Speed Milling Modes for Titanium Alloy Parts," in *XXXV International Scientific and Practical Conference "Problems of Technical and Physical-Mathematical Sciences in Light of Modern Research"*, Novosibirsk, Russia, 2021.
- [19] J. G. R., "A Constitutive Model and Data for Metals Subjected to Large Strains, High Strain Rates and High Temperatures," in *7th International Symposium on Ballistics*, The Hague, Netherlands, 1983.
- [20] P. Vishwakarma and A. Sharma, "3D Finite Element Analysis of milling process for non-ferrous metal using deform-3D," in *10th International Conference of Materials Processing and Characterization*, Mathura, India, Feb. 2020, <https://doi.org/10.1016/j.matpr.2019.12.131>.
- [21] S. Stebunov, A. Vlasov, and N. Biba, "Prediction of fracture in cold forging with modified Cockcroft-Latham criterion," in *17th International Conference on Metal Forming*, Toyohashi, Japan, Sept. 2018, <https://doi.org/10.1016/j.promfg.2018.07.264>.
- [22] I. Ullah, S. Zhang, and S. Waqar, "Numerical and experimental investigation on thermo-mechanically induced residual stress in high-speed milling of Ti-6Al-4V alloy," *Journal of Manufacturing Processes*, vol. 76, pp. 575–587, Apr. 2022, <https://doi.org/10.1016/j.jmapro.2022.02.039>.
- [23] S. Kumar Khare and G. Singh Phull, "Analysis and optimization of cutting parameters under high-speed machining of Ti-6Al-4V alloy," in *International Conference on Materials, Processing & Characterization (13th ICMPC)*, Telangana, India, 2022, <https://doi.org/10.1016/j.matpr.2022.04.613>.